Innovative Infrastructure Solutions (2023) 8:320
https://doi.org/10.1007/s41062-023-01279-3

PRACTICE-ORIENTED PAPER

Enhancing corrosion resistance in reinforced concrete structures by using innovative eco-friendly composite pigments

Walaa M. Abd El-Gawad[1] · Essam A. Mossalam[2] · Mahmoud Gharieb[2]

Received: 1 December 2022 / Accepted: 13 October 2023 / Published online: 10 November 2023

Abstract

This is the first study to look into the use of modified feldspars as anticorrosive pigments in the coatings industry. Herein, novel anticorrosive composite pigments were prepared by the chemical deposition of thin films of different oxides (e.g., zinc oxide and vanadium oxide with doloresite phase) on the surface of feldspar, which comprises 80% of the whole structure. A new vanadium oxide (e.g., doloresite) was chosen due to its IV oxidation state and excellent anticorrosive characteristics. ZnO is also well-known for its high resistance to corrosion. Firstly, the synthesis of the composite pigments was done, and then, they were characterized via XRD, SEM/EDX, XRF, and TGA. The composite pigments were incorporated into solvent-based epoxy coatings to evaluate their anticorrosive performance on reinforced concrete steel. Their corrosion resistances were determined using linear polarization resistivity and electrochemical impedance spectroscopy techniques. The physico-mechanical properties of the dry coats containing the prepared composite pigments were also evaluated. The results revealed that the polarization resistivity (R_{po}) of coatings containing Zn/F ranged from 5900 to 3900 Ohm.cm^2 and that of *V*/*F* ranged from 7077 to 5500 Ohm.cm^2, while the resistivity of uncoated rebar was from 1900 to 1300 Ohm.cm^2. These results confirm that these novel pigments (e.g., ZnO/feldspar and doloresite/feldspar) could provide high corrosion resistivity for concrete structures that are immersed in chloride-laden environments. These composite pigments will be eco-friendly with a low impact on humans and the environment as they contain very low concentrations of heavy metals, besides their high efficiency and economic feasibility.

Keywords Feldspar · Zinc oxide · Vanadium oxide · Novel anticorrosive pigments · Reinforced concrete steel · Coating

Introduction

Corrosion of reinforced concrete steel is regarded as one of the most severe implications for diminishing the durability and service life of reinforced concrete buildings [1, 2]. The most prevalent cause of corrosion is the intrusion of carbon dioxide and chloride ions into the concrete. Chloride ions can erode the passive layer on reinforcing steel and trigger localized corrosion [3]. Simultaneously, carbon dioxide reduces the pH of the concrete, accelerating corrosion. Under vigorous attack, the accumulated corrosion products induce concrete cracking, delamination, and spalling [4]. Consequently, the service life and loading capability of reinforced concrete buildings will be severely damaged. The widespread breakdown of reinforced concrete structures owing to localized corrosion of reinforcing steel causes significant damage. As a result, corrosion and steel protection in concrete became one of the most critical and crucial topics [3, 5]. Steel bars inside concrete that was designed with cement only may be corroded as a result of its high permeability. From the many research studies, the addition of pozzolanic materials to concrete reduced the amount of chloride ions drastically, leading to the hindrance of their diffusion and enhancing the concrete pore structure by decreasing permeability [6–9].

Generally, corrosion inhibition approaches fall into three categories: corrosion inhibitors, cathodic and anodic protection, and organic coatings [10, 11]. The primary goal of using organic coatings is to create a protective layer on the metallic surface, limiting access to corrosive aggressive

✉ Mahmoud Gharieb
medo_20109129@yahoo.com; m.gharieb@hbrc.edu.eg

[1] Polymers and Pigments Department, National Research Centre, Dokki, Cairo, Egypt

[2] Raw Building Materials Technology and Processing Research Institute, Housing and Building National Research Center (HBNRC), Cairo, Egypt

media [12, 13]. Furthermore, when these coatings are exposed to corrosive media, they are unable to provide long-term protection [14, 15]. The application of inhibitors in coating structures limits corrosion reactions. However, utilizing corrosion inhibitors directly in the coating causes several issues, including the degradation of the coating layer, rapid depletion of the inhibitors, and a negative influence on the curing process [16]. To overcome this issue, one of the promising methods employed lately in the literature is the incorporation of inhibitive pigments into the coatings. The development of corrosion inhibition pigments is a feasible method for generating partial solubility in corrosive electrolytes [17].

Pigments containing chromates and lead are considered the most effective inhibitive pigments. However, the environmental issues and toxicity of these pigments drastically decreased their utilization [18]. Therefore, the researchers endeavored to create new trends to generate novel eco-friendly anticorrosive composite pigments via the precipitation of a thin film of the well-known anticorrosive and expensive pigments on cheap natural ores like feldspar. These composite pigments usually contain low concentrations of heavy metals in addition to their low cost [19].

Zinc oxide is the most popular, well-known, and commonly used white inorganic pigment. It is recognized to have a lot of highly desirable features, which should make it an excellent anticorrosive pigment. It has good inhibitive performance as well as great optical features such as exceptional whiteness, high hiding power, and high absorptive power for ultraviolet light [20, 21].

On the other hand, vanadates have been frequently recommended in chemical surface pretreatments of various alloys due to their excellent corrosion resistance and capacity to increase the surface's adhesive qualities. Vanadium in the 4 + oxidation state can provide good corrosion resistance because of its passivation capacity, as Iannuzzi et al. and Stern et al. discovered that doloresite is a novel vanadium oxide with V in the 4 + oxidation state that has excellent anticorrosive characteristics [22–24].

Feldspars are the most abundant mineral in the earth's crust, accounting for over 58 percent of the composition of various rocks and serving as a significant component in metamorphic, igneous, and sedimentary rocks. Feldspars have attracted extensive interest throughout history due to their abundance in nature. They are anhydrous aluminosilicate minerals rich in Na, K, and Ca that consist of orthoclase, albite, and anorthite minerals, and can appear in various solid solution forms, each according to their microstructure [25]. Feldspars are widely employed as raw materials in a variety of interior and exterior applications due to their distinctive compositional and structural characteristics, as well as their numerous unique properties. Feldspars are used in the production of building materials and tiles, abrasives, glass fibers, adhesive bonding agents, welding rods, and enamel lacquerware [26]. However, their use has expanded to include fillers and extenders in paints, plastics, and rubber. The remarkable features and structural richness of feldspars as minerals attracted numerous researchers and scientists to conduct advanced modifications in feldspar materials to impart new functionalities [27, 28].

The aim of this study was to prepare novel eco-friendly anticorrosive pigments as safe alternatives for the toxic and expensive commercial anticorrosive pigments. The present study intended to generate two novel and eco-friendly anticorrosive pigments (e.g., ZnO/feldspar and doloresite/feldspar) via the deposition of a thin film of ZnO or doloresite on the surface of feldspar, which comprises 80% of the whole structure. These pigments are low in toxicity since they include only 20% functional pigments (ZnO or doloresite) and a low concentration of heavy metal. They were characterized and integrated into epoxy paint formulations to evaluate their possibilities for protecting the reinforced steel in concrete against corrosion.

Experimental part

Materials

Materials used in this investigation are ammonium metavanadate and zinc acetate, which were purchased with a purity of 99% from Alpha Lab and Win Lab, UK, respectively. Feldspar (F) was provided from El-Wahat Region, Giza City, Egypt. Sodium hydroxide with high purity (99%) is obtained from Laboratory Rasyan lab (India). The concrete specimens were made using the concrete mix design given in Table 1, which is formed from CEM I type ordinary Portland cement, coarse dolomite, and fine sand aggregates. Their chemical analyses of raw materials are given in Table 2. All the used pigments, extenders, and solvents were of normal chemical grades and were products of different local and international companies.

Table 1 Mix proportions for concrete per 1 m^3

Concrete ingredients, (Kg/m^3)					
Portland cement, CEM 1—42.5N	Water	Sand	Dolomite	Super-plasticizer	Slump (mm)
400	140	632	1264	8	12

Table 2 Chemical composition of ordinary Portland cement (OPC), coarse dolomite and fine sand aggregates (%)

Oxide content	CEM I 42.5N. %	Dolomite	Sand
SiO_2	21.50	1.67	94.40
Al_2O_3	3.47	0.08	2.03
Fe_2O_3	3.39	0.01	0.98
CaO	61.72	35.44	0.71
MgO	1.15	17.51	0.25
SO3–	2.57	0.13	0.30
Cl–	0.09	1.01	0.08
L.O.I	4.53	45.99	0.74
Na_2O	0.30	0.04	0.38
K_2O	0.30	0.02	0.65
TiO_2	–	0.01	0.13
P_2O_5	–	0.01	0.06
MnO	–	–	0.03
Total	99.87	99.97	99.92
Ins. res	0.52	–	–
Na_2OEq	0.51	–	–
L.S.F	0.90	–	–
C3A	2.52	–	–
C3S	52.47	–	–
C2S	22.13	–	–
C4AF	11.51	–	–

Synthesis of ZnO/feldspar (Zn/F) and doloresite/feldspar (V/F) via co-precipitation method

ZnO/feldspar (Zn/F)

Zinc acetate was utilized to precipitate a thin layer of ZnO on the surface of feldspar by using sodium hydroxide to complete the precipitation step until pH = 9. The precipitate was washed, dried, and calcinated at 500 °C for 2 h.

Doloresite/ feldspar(V/F)

Ammonium meta-vanadate was used for the deposition of doloresite, which is a new vanadium oxide with oxidation no. + 4, on the surface of feldspar by adding sodium hydroxide till pH = 9. The precipitate was washed, dried, and calcinated at 500 °C for 2 h. A schematic diagram shown in Fig. 1 represents the synthesis of Zn/F and V/F via the co-precipitation method**.**

Methods of instrumental analysis

In this work, the shape of the particles and the element and oxide concentrations of the prepared composite pigments were determined using energy-dispersive X-ray analysis (EDX) and scanning electron microscopy (SEM) models: the JX 2840 micro-analyzer electron probe, Japan, and an Axios sequential WD X-ray fluorescence (XRF) spectrometer, PANalytical 2005, USA. Additionally, the thermal stability of pigments was investigated via the Perkin Elmer Thermogravimetric analyzer TGA7 technique, USA. Moreover, X-ray powder diffraction patterns were obtained at room temperature using Philip's diffractometer (Model PW1390), employing Ni-filtered Cu Kα radiation ($\lambda = 1.5404$ Å). The diffraction angle, 2θ, was scanned at a rate of 2°/min.

Paints preparation

Both ZnO/feldspar (Zn/F) and doloresite/feldspar (V/F) were integrated into two formulations based on epoxy resin. The pigment/binder ratio of the mix is 2.125, and the paints were prepared using a ball mill. Table 3 presents the formulations.

Reinforced bars preparation

Deformed steel rebars with the chemical composition shown in Table 4 were made by removing contaminants such as mill scales, grease, rust, oil, and dirt using emery sheets. Then, the rebars were cleaned with solvent and dried. After that, the coatings were applied to the rebar surfaces using a brush. The dry film thickness should be adjusted between 100 and 150 μ [29].

Corrosion testing

Several electrochemical measurements (ASTM G1), such as open circuit voltage (OCV) (ASTM C 876), liner polarization resistivity (LPR) (ASTM G5), and electrochemical impedance measurements (EIS) (ASTM 106), were carried out utilizing a biologic potentiostat with the help of EC-Lab software, which was created and constructed to operate a multichannel SP-150. The different electrochemical measurements were carried out in a three-electrode cell configuration consisting of Ag/AgCl as the reference electrode, a platinum spiral as the counter electrode, and reinforced steel bars coated with epoxy-based coatings containing the prepared composite pigments as the working electrode.

- OCV is the variation in electrical voltage between two terminals (positive and negative) of a device when disconnected from any circuit. There is no external load connected, and no external current flows between the terminals.
- LPR is mostly utilized in corrosion monitoring; the polarization resistance (R_p), corrosion current density (I_{corr}), and corrosion rate (C_R) of the materials can be obtained by conducting Tafel plots at scan rates of 0.166 mV s^{-1} according to ASTM G5.

Fig. 1 A schematic diagram of the preparation process

- EIS measurements were carried out in the frequency range of 100 kHz–10 MHz using an alternative current (AC) over potential with an amplitude of 10 mV under the principles of EIS investigation of a high resistance coating.

Mechanical properties of the coatings

The elasticity, strength, and flexibility of the coated films were evaluated according to ASTM as, e.g., hardness [ASTM D 6577], impact resistance [ASTM D2794],

Table 3 The paint formulations

Paints Ingredients (gm)	Feldspar (F)	ZnO/feldspar (Zn/F)	Doloresite/ feldspar (V/F)
Epoxy resin	32	32	32
Fe_2O_3	2	2	2
TiO_2	3	3	3
Kaolin	5	5	5
Feldspar (F)	58	–	–
ZnO/feldspar (Zn/F)	–	58	–
Doloresite/ feldspar (V/F)	–	–	58
Total pigment	68		
Total	100		
P/B	2.125		

ductility [ASTM D 5638], and pull-off strength [ASTM D4541].

Results and discussion

Characterization of the composite pigments

X-ray diffraction

As shown in Fig. 2, XRD was utilized to discover the crystalline phase that is available in feldspar and the prepared composite pigments. XRD pattern of the feldspar showed that feldspar is a mixed mineral composed of albite and quartz. XRD demonstrated intense sharp peaks at low-angle positions ranging from $2\theta = 25$ to 30. The presence of single and sharp peaks described the crystalline structure, which has consistent diameter pores in the range of mesopores. Many tight diffraction peaks in feldspar and the composite pigment patterns revealed their single phase of a highly ordered structure. In the case of the prepared composite pigments, characteristic peaks for ZnO appeared at $2\theta = 31.8°$, 34.5°, 36.2°, and 47.7°, while characteristic peaks for vanadium oxide (doloresite) appeared at $2\theta = 19°$, 23.2°, 30°, 36.5°, 41.5°, 46°, and 46.5°. XRD diffraction of V/F showed that

Table 4 Chemical analysis of reinforcing steel, (%)

Chemical analysis of steel (%)											
C	Si	Mn	P	S	Cr	Ni	Cu	Mo	Al	Fe	Total
0.088	0.063	0.590	0.015	0.021	0.124	0.125	0.253	0.022	0.011	98.60	99.535

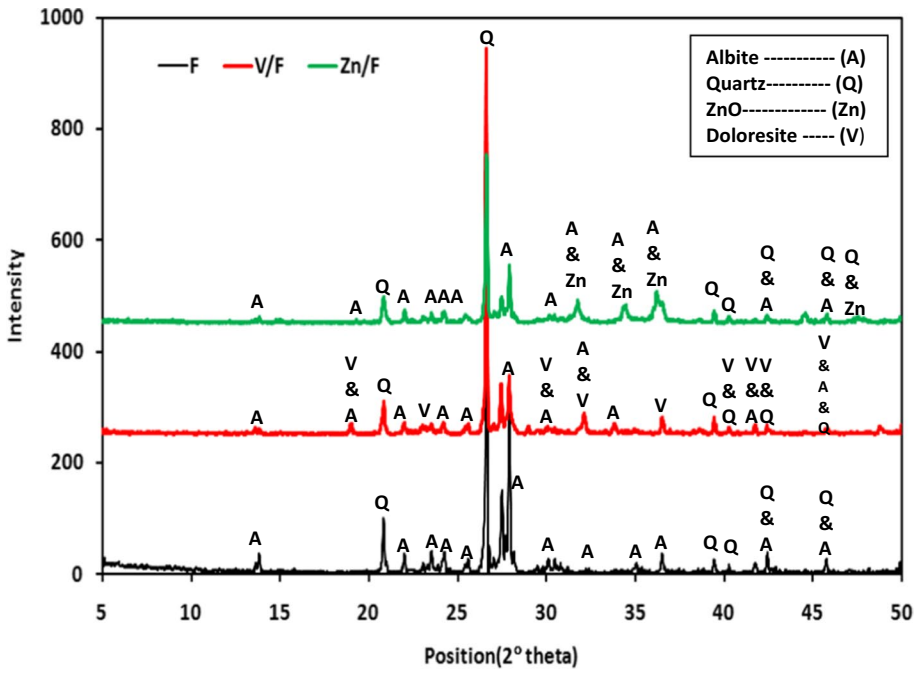

Fig. 2 XRD charts of the prepared composite pigments

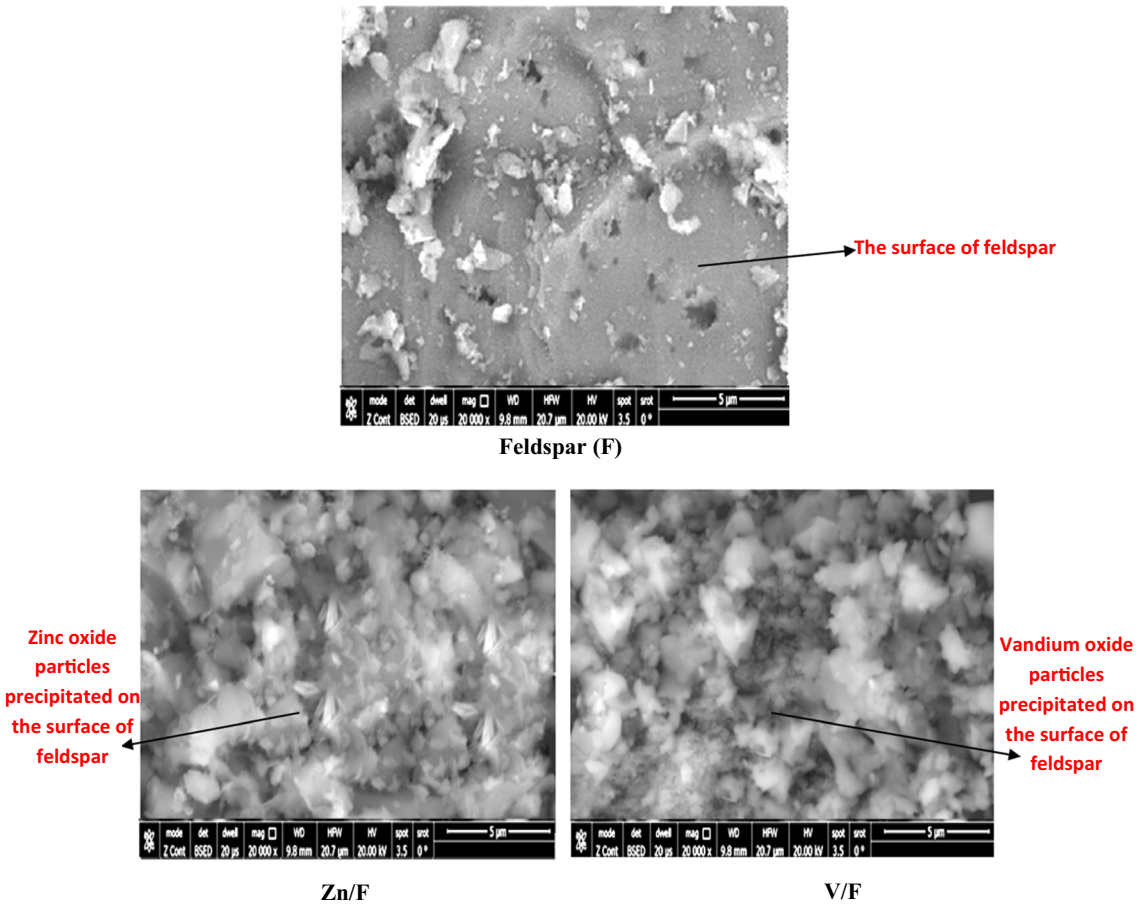

Fig. 3 SEM photographs of the prepared composite pigments

the doloresite phase of vanadium oxide was formed, which is an advantage as doloresite is a novel vanadium oxide with V in the 4 + oxidation state that has excellent anticorrosive characteristics.

SEM

SEM photographs of feldspar and the prepared composite pigments are shown in Fig. 3. SEM photograph of feldspar showed that its particles are very large, blocky, and have dissolution cavities. SEM photographs of the composite pigments exhibited that small particles of ZnO and doloresite covered the surface of feldspar, and these particles filled the cavities. Thus, by the deposition of zinc oxide or doloresite on the surface of feldspar, more compact skeletal feldspar is formed, and the disappearance of the cavities of the feldspar layers was observed [30].

EDX analysis

The elements of ZnO and doloresite deposited on the surface of the feldspar up to 1 μ depth were investigated using EDX analysis, as presented in Fig. 4. In the case of Zn/F composite pigment, the characteristic elements of ZnO, which are Zn and O, appeared besides elements of feldspar (e.g., Si, Al, Na, and K). It is noticeable that the concentration of Zn is very low, which proves the deposition of a thin layer of ZnO on the surface of feldspar, while V and O appeared with a low ratio in V/F composite pigments in addition to Si, Al, Na, and K elements of feldspar. The results shown here prove the successful precipitation of a thin layer of expensive functional oxides (ZnO and doloresite) on the surface of a cheap and readily available natural ore (feldspar).

X-ray fluorescence analysis

The XRF analysis illustrated in Table 5 shows the concentration of the oxides in feldspar and the composite pigments. The results deduced that feldspar is mainly composed of SiO_2, Al_2O_3, Fe_2O_3, Na_2O, and K_2O, with traces of other oxides. On the other hand, XRF results of the prepared pigments showed the appearance of zinc oxide or vanadium oxide with a ratio of nearly 20% of the whole components,

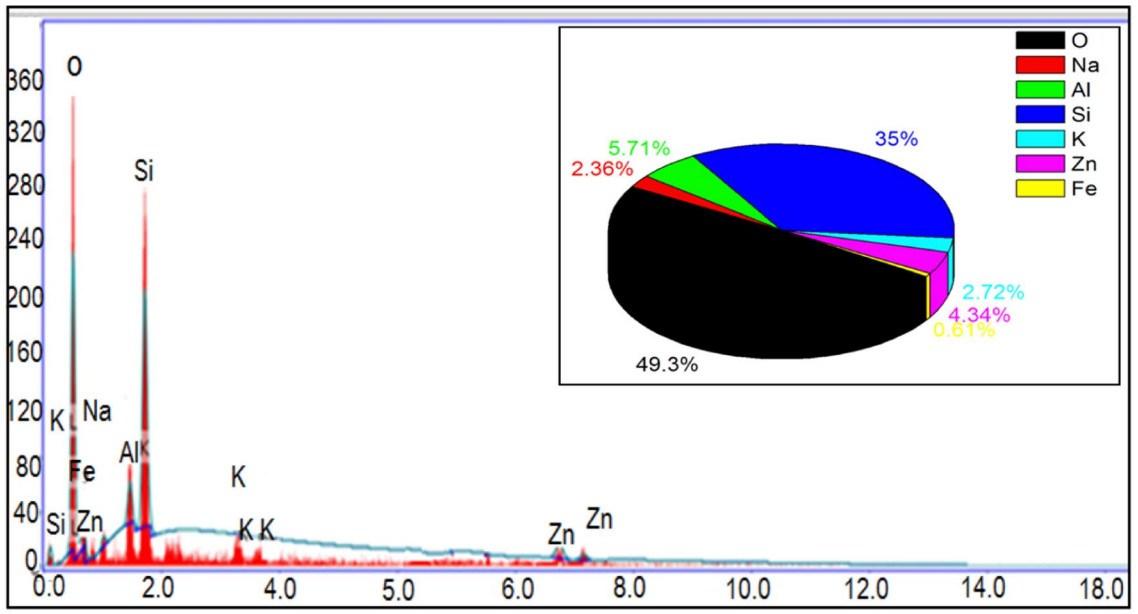

Zn/F

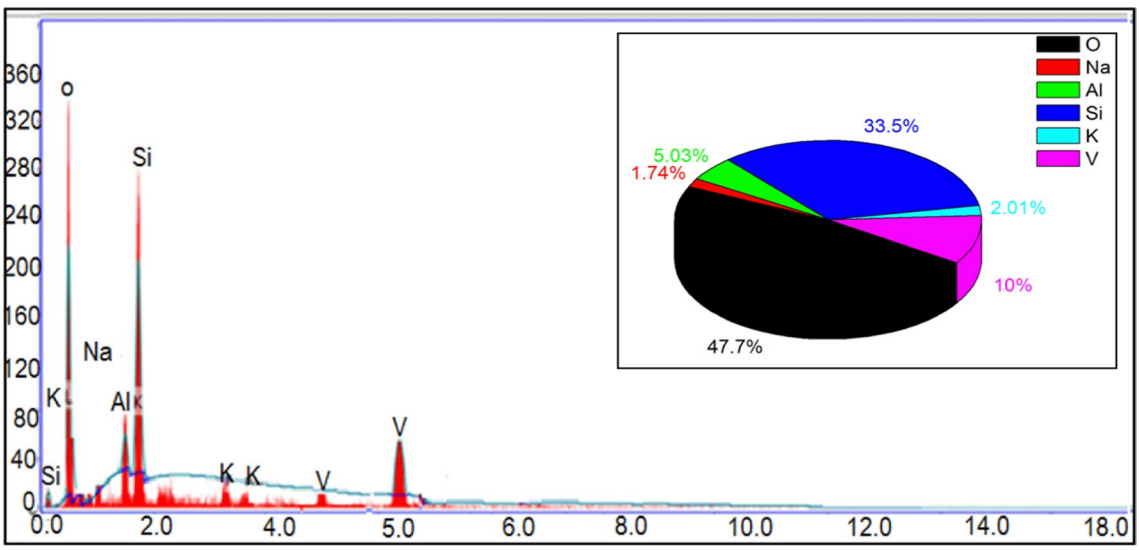

V/F

Fig. 4 EDX analysis of the prepared composite pigments

Table 5 XRF analysis

Main constituents (wt%)	SiO_2	Al_2O_3	Fe_2O_3	CaO	MgO	SO_3	Na_2O	K_2O	TiO_2	P_2O_5	ZnO	$V2O_5$	LOI
Feldspar (F)	78.54	9.94	0.86	1.36	0.10	0.03	4.21	4.44	0.07	0.01	91.5	–	0.44
ZnO/feldspar (Zn/F)	64.55	7.25	0.49	1.10	0.07	0.01	2.92	2.66	0.04	–	20.80	–	0.11
Doloresite/ feldspar (V/F)	64.72	7.92	0.52	1.08	0.09	0.01	3.10	2.84	0.06	0.007	–	19.64	0.013

in addition to the oxides existing in feldspar. This validates the results of the EDX analysis, which demonstrated the successful deposition of thin shells of zinc oxide or vanadium oxide on the surface of feldspar.

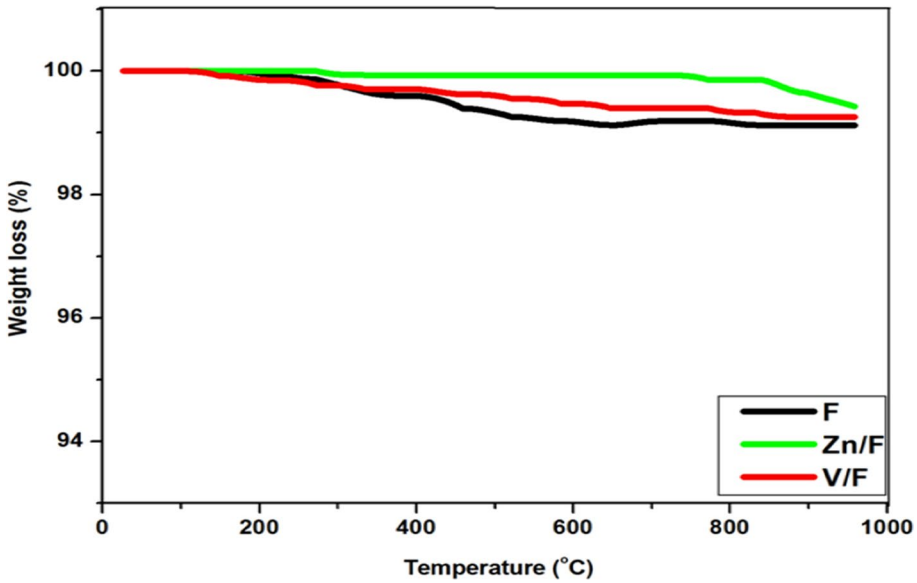

Fig. 5 TGA of the prepared composite pigments

TGA analysis

The thermogravimetric curves for feldspar and the composite pigments are represented in Fig. 5. The thermal pattern of feldspar contains one weight loss at about 570 °C, which is attributed to the decomposition of quartz. The TGA curves of the composite pigments appeared to have a lower weight loss than feldspar, which means that the deposition of ZnO and doloresite on the surface of feldspar enhanced the thermal stability.

Investigating corrosion resistance reinforced concrete steel coated with epoxy coatings containing Zn/F and V/F composite pigments

OCP measurements

Table 6 indicates several electrochemical parameters such as polarization resistance (R_{Po}), the corrosion current density (I_{corr}), and corrosion rate (C_R) obtained after immersion of two reinforced concrete steel bars painted with a coating containing V/F and Zn/F, besides uncoated rebar (control) in 3.5% NaCl for 28 days, via fitting the Tafel plots (linear polarization curves) exhibited in Fig. 6 at a scan rate of 0.166 mV s^{-1}

The results showed that the I_{corr} and C_R values of uncoated reinforced concrete steel (control) are 38 µA/cm^2 and 34 µm/year, respectively. These values are very high, so the resistance of control is low (1367 Ohm.cm^2). The I_{corr} and C_R values of reinforced concrete steel coated with V/F were 0.072 µA/cm^2 and 1.3 µm/year, respectively, indicating that its resistance was high (5967 Ohm.cm^2). These results deduce that the resistance of reinforced concrete steel coated with *V/F* was the best, offering a high R_{Po} and, accordingly, a low I_{corr} and C_R, followed by that of steel coated with Zn/F, and control was the least. This is attributed to the fact that coating the steel surface with coatings containing the prepared composite pigments can decrease the porosity and accordingly reduce the permeability, consequently reducing the current density and the corrosion rate. Moreover, the positive shift in the value of E_{ocv} of reinforced concrete steel coated with V/F and Zn/F compared to the uncoated rebar with reference electrode indicates the high corrosion resistance (R_p) provided by coated rebars based on V/F and Zn/F.

Table 7 presents a broad criterion for corrosion that has been developed from field and laboratory investigations [31, 32]. By comparing the results of the present work and the results of the literature review, it can be noticed that the corrosion resistance of the prepared pigments is high and in good agreement with the standard methods.

Table 6 Electrochemical measurements results obtained from potentiodynamic anodic polarization and OCV Technique

Concrete mix	Corrosion Current density I_{corr} (µA/cm^2)	Corrosion potential E_{corr} (mV)	Corrosion rate CR (µm/year)	Concrete resistivity Rpo (Ohm.cm^2)
Control	38	− 760	34	1367
Zn/F	1.6	− 309	1.9	4400
V/F	0.072	− 266	1.3	5967

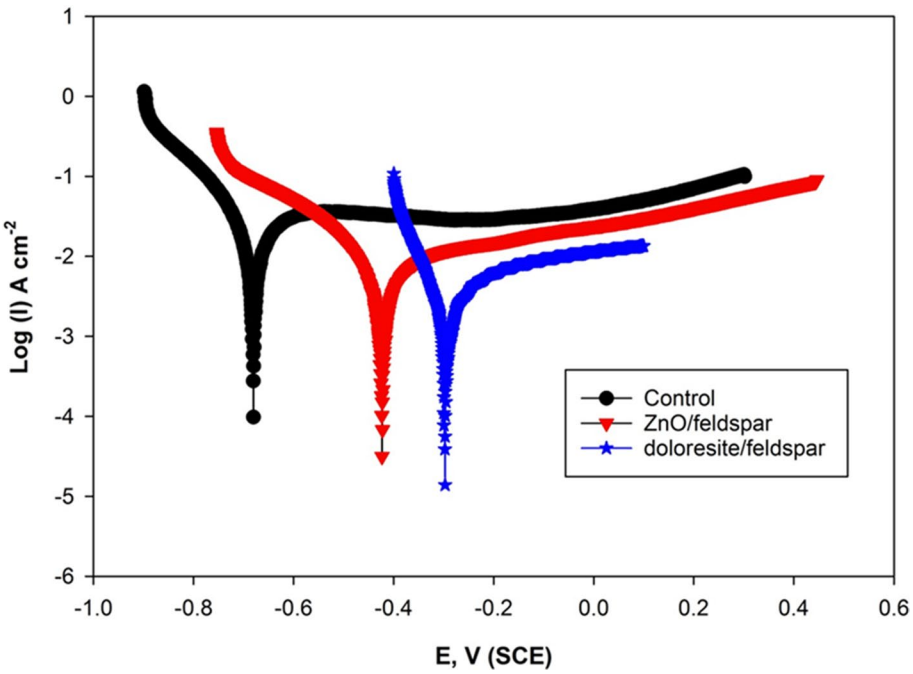

Fig. 6 Tafel plots

Table 7 Corrosion risk for steel in concrete as assessed from polarization resistance, corrosion current density and corrosion rate measurements

Corrosion risk	Polarization resistance, RP (kΩ cm^2)	Corrosion Current density, Icorr (μA/cm^2)	Corrosion rate, (μm/year)
Very high	2.5–0.25	10–100	100–1000
High	25–2.5	1–10	10–100
Low/moderate	250–25	0.1–1	1–10
Passive	> 250	< 0.1	< 1

EIS measurements

To further check the effect of coatings containing Zn/F and V/F on the resistance of reinforced concrete steel, the EIS technique was employed through immersion in 3.5% NaCl for 28 days. In this way, Nyquist plots recorded for the three reinforced concrete rebars are depicted in Fig. 7. Table 8 represents the extracted electrochemical elements.

The semi-circle curve in Nyquist plots is mostly relevant to inhibitor corrosion protection performance. Notably, the diameter of the semi-circle would have increased as the passively adsorbed layers became more homogeneous and integrated. The resistance of the passively adsorbed layers is proportional to the slopes of semi-circles at medium frequencies. It is worth noting that the double layer's transport mechanism is tightly tied to the low-frequency range [33].

In the case of the uncoated rebars (the control), the results showed an intense drop in the R_{po} values after the immersion for 28 days. This is attributed to the fact that in a short immersion time (i.e., up to 7 days), the chloride ions rarely permeate deeply enough into the concrete to damage the passive film created in the pores, whereas after a long period, more corrosive ions can easily enter the concrete and facilitate galvanic corrosion [33].

In the case of rebars embedded in coatings containing Zn/F and V/F composite pigments, the Nyquist plots displayed in Fig. 7 are split into two semi-circles, the first loop at high frequency and the second at moderate frequency. The initial capacitive loop is hypothesized to be an indicator of the generation of protective porous corrosion products. The second one corresponds to the polarization resistance process at the rebar surface beneath the coating layer. Polarization resistivity (R_{po}) of coatings containing Zn/F ranged from 5900 to 3900 Ohm.cm^2 and that of V/F ranged from 7077 to 5500 Ohm.cm^2, while the resistivity of uncoated rebar was from 1900 to 1300 Ohm.cm^2. Thus, R_{po} values of rebars embedded in coatings containing Zn/F and V/F presented higher R_{po} values than those of the control, which may be due to the lowest current density of the prepared coatings and pitting formation, which needs high anodic potential. The R_{po} values of Zn/F and V/F show how efficiently the passive-adsorbent layers have generated. As the formed complexes are adsorbed on the molecular layer, chlorides are prevented from reaching the surface. The adsorbed molecular layer prevents chlorides from approaching the surface through a physical barrier or electrostatic repulsion [34].

R_{po} values followed the pattern V/F > Zn/F > control (uncoated rebar), as shown in Fig. 8. Longer exposure durations resulted in continued decreases in R_{po} values for

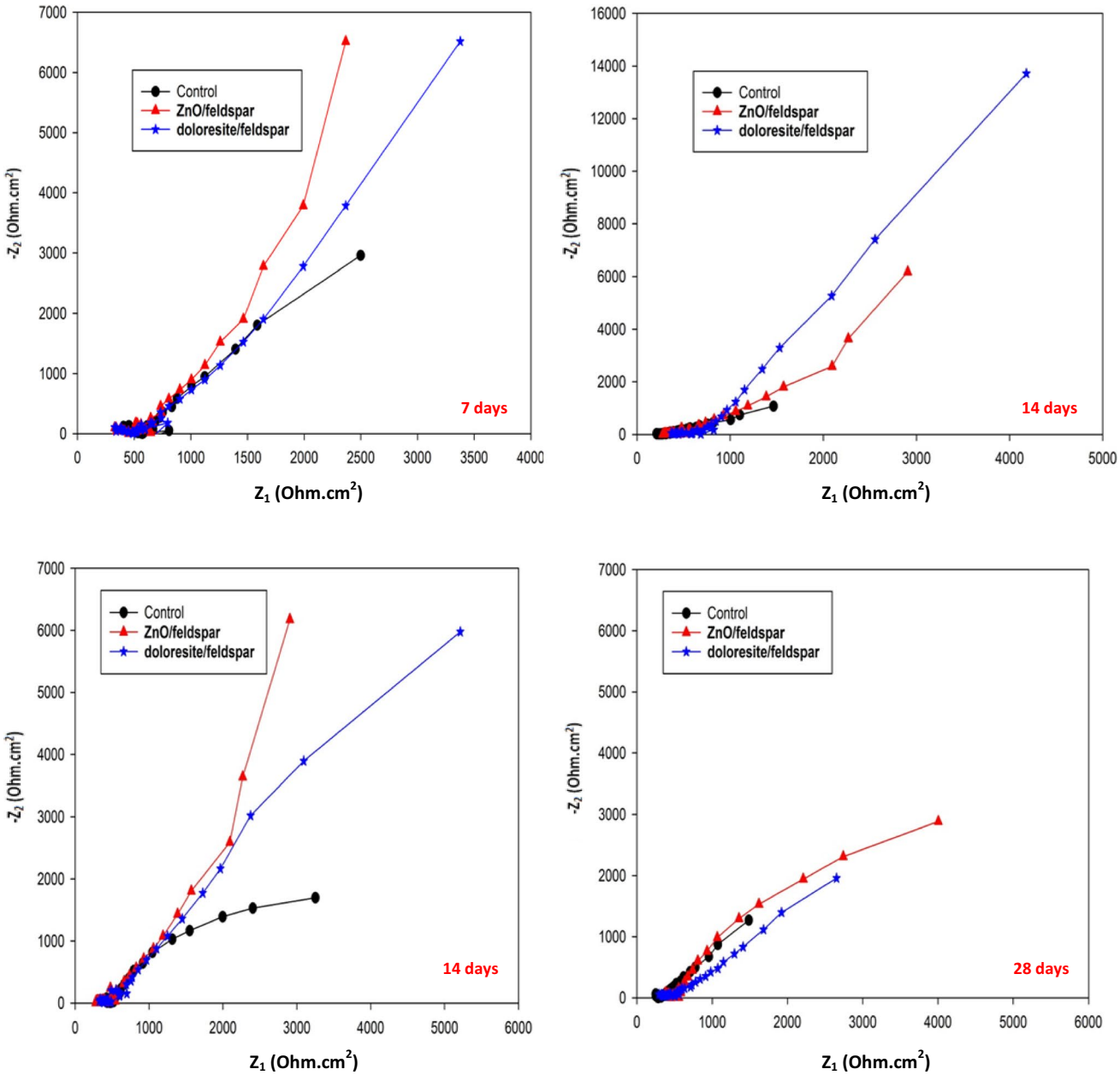

Fig. 7 Nyquist plots

the three rebars. This is because the chloride ions diffuse through the defects and eventually reach the coating/steel contact, where they can initiate the corrosion process. However, R_{po} remains high until the end of the immersion time. After 28 days of immersion, R_{po} was 5500 Ohm.cm^2 for the rebar embedded in a coating containing V/F and 3900 Ohm.cm^2 for that based on Zn/F.

CPE_{dl} values of rebars embedded in Zn/F and V/F coatings were lower than control CPE_{dl} values. This is attributed to the high dielectric constant of Zn/F and V/F molecules replacing the water molecules in the Helmholtz layer. However, in the case of uncoated rebar (control), the exposed area of uncoated rebar will increase and favor the corrosion process.

To quantitatively discuss the results, the impedance data were fitted according to the equivalent simple Randle circuit depicted in Fig. 9, in which the CPE (constant phase element) was utilized rather than the pure capacitor. This is due to the non-homogeneity of the corroding system. R_c and CPE_c denote the resistance and capacitance of coatings and/or concrete, respectively. The CPE_c also reflects a coating's propensity to absorb water. CPE_{dl} and R_{po} are related to the

Table 8 EIS data

Sample	Days	Rc (Ohm.cm^2)	CPEc (farad/cm^2)	Rpo (Ohm.cm^2)	CPEdl (farad cm^{-2} s$^{-(1-\alpha)}$dl)
Control	7 days	852	62.16×10^{-6}	1900	12.81×10^{-6}
	14 days	532	89.94×10^{-6}	1500	22.30×10^{-6}
	21 days	506	12.43×10^{-4}	1400	28.04×10^{-6}
	28 days	428	15.85×10^{-4}	1300	36.25×10^{-6}
Zn/F	7 days	1524	29.35×10^{-6}	5900	3.185×10^{-9}
	14 days	1200	36.98×10^{-6}	4500	4.527×10^{-9}
	21 days	1060	51.03×10^{-6}	4400	4.045×10^{-9}
	28 days	1039	62.45×10^{-6}	3900	6.992×10^{-9}
V/F	7 days	1700	33.07×10^{-6}	7077	1.852×10^{-9}
	14 days	1550	25.82×10^{-6}	6300	2.019×10^{-9}
	21 days	1500	40.02×10^{-6}	5600	3.841×10^{-9}
	28 days	1432	58.94×10^{-6}	5500	3.890×10^{-9}

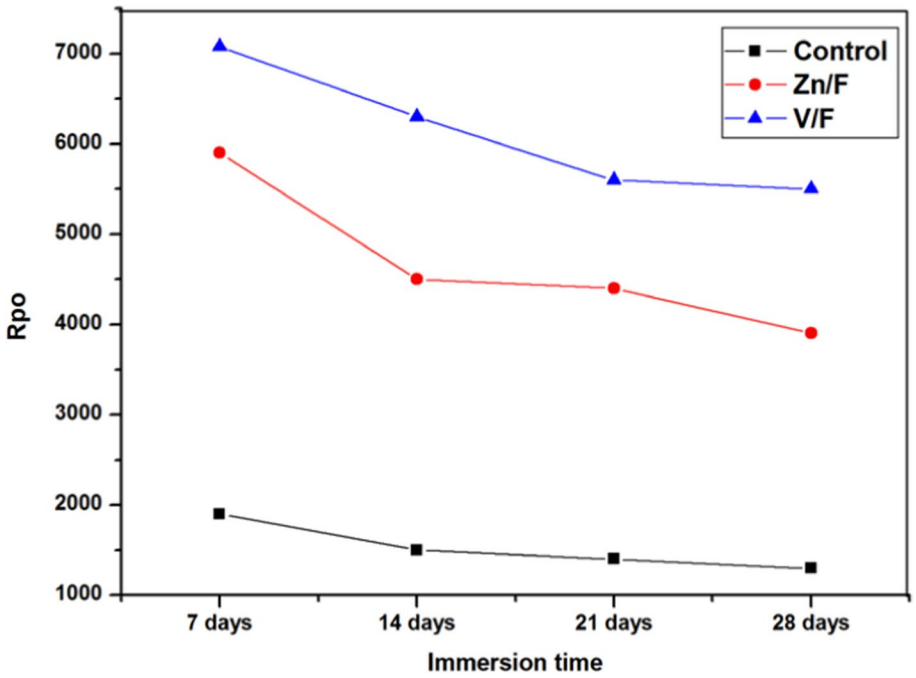

Fig. 8 Rpo values of the three rebars during the immersion time

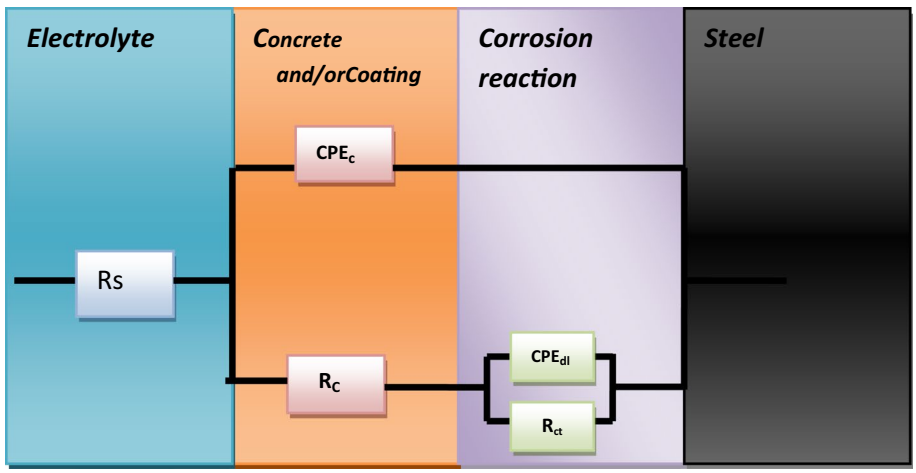

Fig. 9 Equivalent electrical circuit used to fit the EIS data

double-layer capacitance and the corrosion process's charge transfer resistance, respectively. α_{dl} points to the irregularities of the steel surface/electrolyte interface.

Furthermore, it is assumed that epoxy coatings incorporating Zn/F and V/F can establish a protective film on the metallic surface, resulting in a reduced CPE_c layer. Water molecules cannot permeate the surface layer when the layer is thicker and less porous. The good anticorrosive performance of Zn/F and V/F coatings can be attributed to the following assumptions.

Zn cation in Zn/F can be adsorbed onto the steel surface, forming Zn oxide/hydroxide beneath the coatings and passivating the reinforcing steel surface. This assumption implies that the cathodic and anodic sites were protected simultaneously on the steel surface [34].

Coatings based on V(IV) may prevent corrosion via several hydrolysis-condensation-polymerization reactions to form compounds with different molecular weights, along with V(IV) reduction to V(III) at the solution/metal interface. At the beginning of immersion time, the diffusion of water can increase the interfacial pH gradually due to the formation of $VO(OH)_2$ as shown in Eq. 1;

$$VO_2 + 2H_2O \rightarrow VO(OH)_2 + H^+ \quad (1)$$

Moreover, two molecules of $VO(OH)_2$ react again to form condensed $HV_2O_5^-$ as in Eq. (2).

$$2VO(OH)_2 \rightarrow HV_2O_5^- + H^+ + H_2O \quad (2)$$

$HV_2O_5^-$ rapidly polymerizes and forms [–V(IV)–O–V(IV)–] linkages due to the continuous diffusion of water. When the pH of the interfacial area increases, the V(III) species that are predominant should be VO^+ at about millimolar concentrations. After that, the hydrolysis of VO^+ occurs to form VOOH, as exhibited in Eq. (3).

$$VO + + H_2O \rightarrow VOOH + H^+ \quad (3)$$

Generally, at the beginning of corrosion, V(IV) species in coated films can play a significant role in the corrosion resistance of steel by avoiding reduction or hydrolysis to V(III) at the susceptible site and forming gelatinous vanadium hydroxide with the molecular formula $[VO(OH)_2 \cdot nH_2O]$ and $[VOOH \cdot mH_2O]$. Following that, these hydroxides could be condensed to generate polymeric gelation, in which condensed sol molecules gain self-crosslinking through the development of high-density networks. As a result, the produced gels are entrapped in the pores of the coating layers and are enough to provide passivation at the critical site [15]. Figure 10 presents a schematic diagram of the suggested protection mechanism of coatings containing V/F composite pigment.

By summing up all of the above results, it is clear that the two prepared composite pigments can protect reinforced concrete steel from corrosion successfully by forming passive and barrier layers on the steel surface. These layers can restrict the diffusion of corrosive materials in the electrolyte to the active places on the steel surface.

Pull-off test (coating/substrate adhesion strength)

At prolonged immersion times, the coatings could detach and fail. The adhesion of the coatings containing the prepared composite pigments was investigated through a pull-off test for both dry and wet films, as shown in Fig. 11. The results presented show that dry films have better adhesion strength than wet films. However, the wet adhesion strengths of the films are considered good, with high values. The adhesion can be improved via physical mechanisms by interlocking and forming a barrier layer. Herein, by applying coatings containing composite pigments onto the substrates, a barrier compact film with a high build can be formed, hindering the penetration of aggressive materials to the metal/coating interface. That is why the coatings showed good wet adhesion strength during the immersion time. To quantify the coating/substrate adhesion strength after immersion time, the adhesion loss (ψ) values were calculated using the following equation:

$$\psi = \left(\alpha_D - \alpha_W\right)/\alpha_D * 100$$

where α_D is the dry adhesion and α_w is the wet adhesion after 28 days of immersion. The calculations showed that the adhesion loss (ψ) of a coating containing Z/F was 18.75% and that of one containing V/F was 16.84%.

Mechanical properties

Figure 12 illustrates the mechanical properties of coated panels containing the prepared composite pigments. The results deduced that the strength of the coated panels was very high. This may be attributed to the morphology of the prepared composite pigments, as mentioned in the SEM section. SEM photographs of the pigments exhibited that small particles of ZnO and doloresite covered the surface of feldspar and arranged themselves neatly; besides, these tiny particles filled the cavities. Thus, a more compact skeleton of feldspar was formed, which helps in constructing a uniform coat layer with a high build film and high strength. Additionally, it is observed that the ductility and impact resistance values of the coated panels were low. The good arrangement of the different particles with different sizes could hinder the movement of the atoms; therefore, the elasticity of these coatings can be decreased, thus decreasing ductility and impact resistance values.

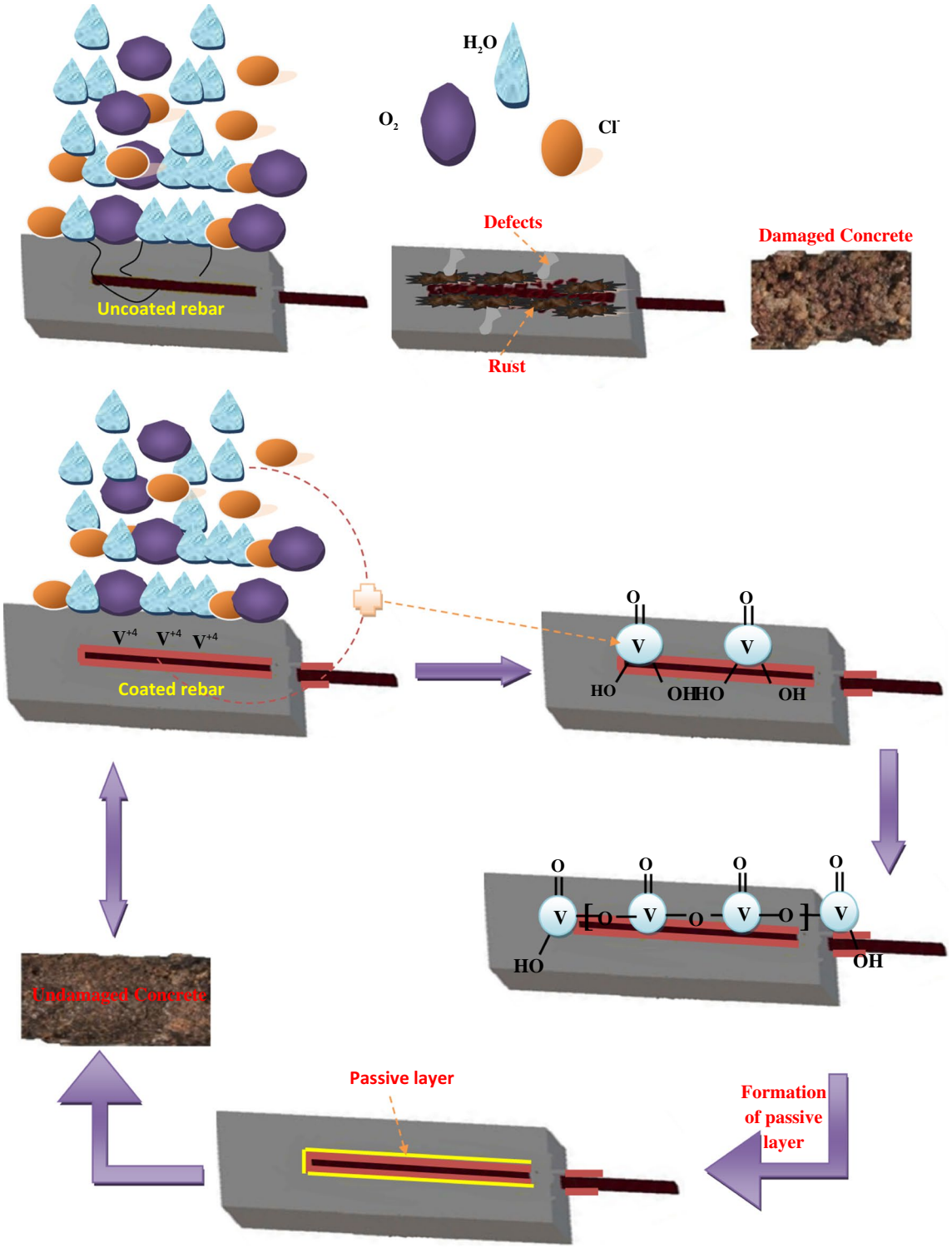

Fig. 10 A schematic diagram of suggested protection mechanism of coatings containing V/F composite pigment

Conclusions

Innovative, cost-effective, and eco-friendly composite pigments based on feldspar (natural ore) as a cheap and safe constituent and a thin shell (e.g., ZnO and vanadium oxide with doloresite phase) were generated to be applied in anti-corrosive coatings. These composite pigments are low in toxicity since they include only 20% functional pigments

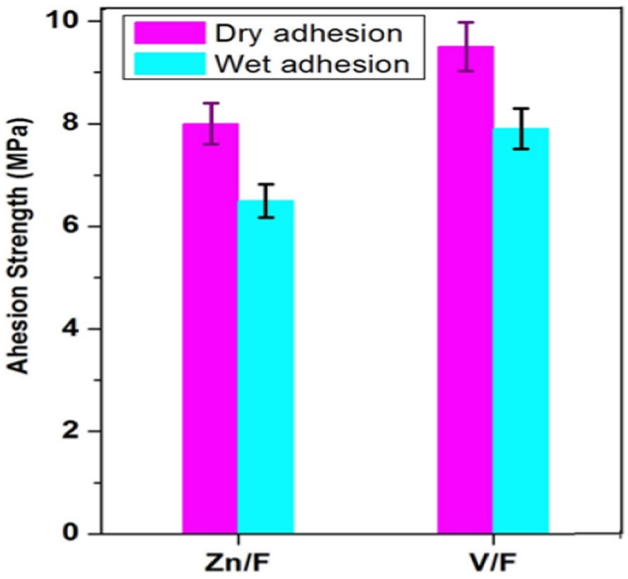

Fig. 11 Pull-off test results

(ZnO or doloresite) and a low concentration of heavy metal. XRD, XRF, SEM/EDX, and TGA techniques were used to confirm the preparation of novel composite pigments. The corrosion protection of the reinforced concrete steel coated with epoxy coatings containing Zn/F and V/F has been explored in a chloride-laden concrete environment, and the following observations have been obtained:

- The open circuit potential results of coatings containing Zn/F and V/F composite pigments showed that potential values became nearly stable after 28 days of immersion. The measured values were E_{corr} − 390 and − 266 mV s^{-1} for Zn/F and V/F, respectively. According to the ASTM C876-standard, there is a possibility lower than 10% for the occurrence of corrosion. Also, the main reason for the better resistance of epoxy-coated rebars than uncoated rebar (control) is the penetration of aggressive materials into the concrete first and then the epoxy matrix.
- After 28 days, the resistance of reinforced concrete steel coated with Zn/F and V/F composite pigments was evaluated by EIS, and the results revealed that the rebars coated with Zn/F and V/F could provide high corrosion resistivity for concrete structures that exist in chloride-laden environments. The polarization resistivity of coating containing Zn/F ranged from 5900 to 3900 Ohm/cm^2 and that of V/F ranged from 707 7 to 5500 Ohm.cm^2, while the resistivity of uncoated rebar was from 1900 to 1300 Ohm.cm^2. The data proved the formation of a protective passive layer on the reinforcing steel surface.
- As a result, it can be concluded that the inclusion of Zn/F and V/F into coatings can help in decreasing the formation of expansive corrosion products on steel rebar surfaces. The good corrosion resistance of coatings containing Zn/F and V/F composite pigments gives rise to a remarkable increase if compared with uncoated rebars after exposure to 3.5% NaCl solution for a long time.

Funding Open access funding provided by The Science, Technology & Innovation Funding Authority (STDF) in cooperation with The Egyptian Knowledge Bank (EKB).

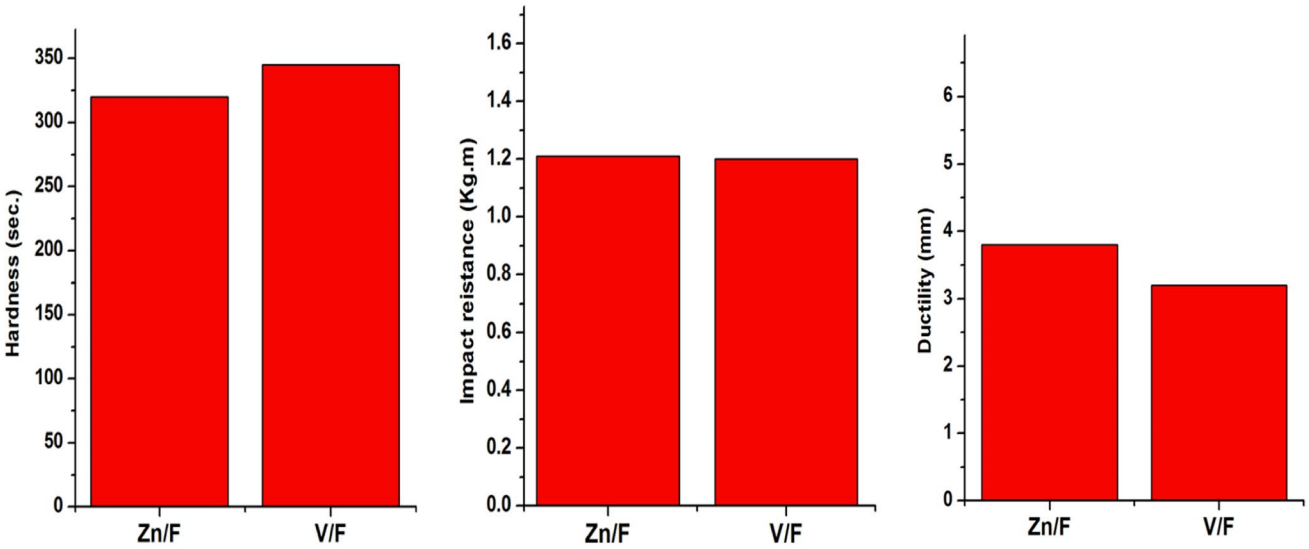

Fig. 12 Physico-mechanical properties of coatings containing the prepared pigments

Declarations

Conflict of interest The authors declare that they have no known competing financial interests or personal relationships that could have appeared to influence the paper.

Ethics approval Not applicable.

Informed consent Not applicable.

Consent for publication Not applicable.

References

1. Wei A, Tan MY, Koay Y, Hu X, Al-Ameri R (2021) Effect of carbon fiber waste on steel corrosion of reinforced concrete structures exposed to the marine environment. J Clean Prod 316:128356
2. Liu Y, Song Z, Wang W, Jiang L, Zhang Y, Guo M, Song F, Xu N (2019) Effect of ginger extract as a green inhibitor on chloride-induced corrosion of carbon steel in simulated concrete pore solutions. J Clean Prod 2019(214):298–307
3. Wang X, Shao M, Ye C, Dong S, Du R, Lin C (2021) Study on effect of chloride ions on corrosion behavior of reinforcing steel in simulated polluted concrete pore solutions by scanning micro-reference electrode technique. J Electroanal Chem 895:115454
4. Yang H, Xiong C, Liu X, Liu A, Li T, Ding R, Shah SP, Li W (2021) Application of layered double hydroxides (LDHs) in corrosion resistance of reinforced concrete-state of the art. Constr Build Mater 307:124991
5. Guler S, Türkmenoglu ZF, Ashour A (2020) Performance of single and hybrid nanoparticles added concrete at ambient and elevated temperatures. Constr Build Mater 250:118847
6. Ghouchani K, Abbasi H, Najaf E (2022) Some mechanical properties and microstructure of cementitious nanocomposites containing nano-SiO_2 and graphene oxide nanosheets. Case Stud Construct Mater 17:e01482
7. Najaf E, Abbasi H (2022) Using recycled concrete powder, waste glass powder, and plastic powder to improve the mechanical properties of compacted concrete: cement elimination approach. Adv Civ Eng 2022:1–12. https://doi.org/10.1155/2022/9481466
8. Najaf E, Abbasi H (2022) Impact resistance and mechanical properties of fiber-reinforced concrete using string and fibrillated polypropylene fibers in a hybrid form. Int Feder Struct Concrete 24:1–14. https://doi.org/10.1002/suco.202200019
9. Najaf E, Orouji M, Ghouchani K (2022) Finite element analysis of the effect of type, number, and installation angle of FRP sheets on improving the flexural strength of concrete beams. Case Stud Construct Mater 17:e01670
10. Mousavifard SM, Nouri PMM, Attar MM, Ramezanzadeh B (2013) The effects of zinc aluminum phosphate (ZPA) and zinc aluminum polyphosphate (ZAPP) mixtures on corrosion inhibition performance of epoxy/polyamide coating. J Ind Eng Chem 19:1031–1039
11. Rani EA, Basu BBJ (2012) Green inhibitors for corrosion protection of metals and alloys: an overview. Int J Corros. https://doi.org/10.1155/2012/380217
12. Hamadi L, Mansouri S, Oulmi K, Kareche A (2018) The use of amino acids as corrosion inhibitors for metals: a review. Egypt J Pet 27:1157–1165
13. Alibakhshi E, Ghasemi E, Mahdavian M, Ramezanzadeh B (2016) Corrosion inhibitorrelease from Zn–Al–[$PO4^{3-}$]–[CO_3^{2-}] layered double hydroxide nanoparticles. Prog Color Color Coat 2016:233–248
14. Harvey TJ, Walsh FC, Nahle AH (2018) A review of inhibitors for the corrosion of transition metals in aqueous acids. J Mol Liq 266:160–175
15. Rao BVA, Rao MV, Rao SS, Sreedhar B (2013) Surface analysis of carbon steel protected from corrosion by a new ternary inhibitor formulation containing phosphonated glycine, Zn^{2+} and citrate. J Surf Eng Mater Adv Technol 3:28–42
16. Kusmierek E, Chrzescijanska E (2015) Tannic acid as corrosion inhibitor for metals and alloys. Mater Corros 66:169–174
17. Moghaddam PN, Amini R, Kardar P, Ramezanzadeh B (2021) Epoxy-ester coating reinforced with cerium (III)-tannic acid-based hybrid pigment for effective mild-steel substrate corrosion protection. Prog Org Coat 161:106485
18. Ahmed NM, Abd El-Gawad WM, Youssef EA, Souaya ER (2016) Study on the corrosion protection performance of new ferrite/kaolin core-shell pigments in epoxy-based paints. Anti-Corros Methods Mater 63:1–11
19. Ahmed NM, Fathi AM, Mohamed MG (2020) Abd El-Gawad WM Evaluation of new core-shell pigments on the anticorrosive performance of coated reinforced concrete steel. Prog Org Coat 140:105530
20. Heydari V, Bahreini Z (2018) Synthesis of silica-supported ZnO pigments for thermal controlcoatings and analysis of their reflection model. J Coat Technol Res 15:223–230
21. Xu X, Wang H, Wu J, Chen Z, Zhang X, Li M (2022) Hydrothermal in-situ synthesis and anti-corrosion performance of zinc oxide hydroxyapatite nanocompositeanti-corrosive pigment. Coatings 12:420
22. Gao Z, Zhang D, Hou L, Li X, Wei Y (2019) Understanding of the corrosion protection by V(IV) conversion coatings from a sol-gel perspective. Corros Sci 161:108196
23. Iannuzzi M, Frankel GS (2007) Mechanisms of corrosion inhibition of AA2024-T3 by vanadates. Corros Sci 49:2371–2391
24. Stern TW, Stieff LR, Evans HT Jr, Sherwood AM (1957) Doloresite, a new vanadium oxide mineral from the Colorado Plateau. Am Mineral 42:587–593
25. Fuertes V, Reinosa JJ, Fernandez JF, Enríquez E (2022) Engineered feldspar-based ceramics: a review of their potential in ceramic industry. J Eur Ceram Soc 42:307–326
26. Kim J, Lee J, Kim Y, Kim D, Kim J, Han J (2022) Evaluating the eco-compatibility of mortars with feldspar-based fine aggregate. Case Stud Constr Mater 16:e00781
27. Bagheri M, Lothenbach B, Shakoorioskooie M, Scrivener K (2022) Effect of different ions on dissolution rates of silica and feldspars at high pH. Cem Concr Res 152:106644
28. Ali BJ, Othman SS, Harun FW, Jumal J, Abdul Rahman MB (2018) Immobilization of enzyme using natural feldspar for use in the synthesis of oleyloleate. AIP Conf Proc 1972:030018

29. Gharieb M, Mosleh YA, Rashad AM (2021) Properties and corrosion behavior of applicable binary and ternary geopolymer blends. Int J Sustain Eng 14(5):1068–1080
30. Yakicier C, Tuncer M, Aydin N, Akarsu N (2008) Environmental effect and genetic influence: A regional cancer predisposition survey in the Zonguldak region of Northwest Turkey. Environ Geol 54:391–409
31. Rilem TC (2004) 154-EMC. Electrochemical techniques for measuring metallic corrosion' test methods for on-site corrosion rate measurement of steel reinforcement in concrete by means of the polarization resistance method. Mater Struct Matériauxet Construct 37:623–643
32. ASTM C876 (1999) Standard test method for half-cell potentials of uncoated reinforcing steel in concrete. ASTM International, West Conshohocken
33. Teymouri F, SamieiI ASR, Azamian I, Johari M, Shekarchi M (2022) Passive film alteration of reinforcing steel through $[MoO_4^{2-}]/[RCOO^-]$ interfacial co-interaction for enhanced corrosion resistance in chloride contaminated concrete pore solution. J Mol Liq 356:119060
34. Mohamed MG, Ahmed NM, Abd El-Gawad WM (2018) Corrosion protection performance of reinforced steel coated with paints based on waste materials. Anti-Corros Methods Mater 65:368–374